The Canadian Mineralogist
Vol. 42, pp. 1859-1870 (2004)

EXSOLUTION IN NIOBIAN RUTILE FROM THE PEGMATITE DEPOSIT AT GREENBUSHES, AUSTRALIA

MARIANA KLEMENTOVÁ[§] AND MILAN RIEDER[¶]

Institute of Geochemistry, Mineralogy and Natural Resources, Faculty of Science,
Charles University, Albertov 6, CZ–128 43 Prague, Czech Republic

ABSTRACT

Niobian rutile $(Ti^{4+}_{0.63}\,Nb^{5+}_{0.14}\,Fe^{2+}_{0.11}\,Ta^{5+}_{0.08}\,Fe^{3+}_{0.02}\,W^{6+}_{0.01}\,Sn^{4+}_{0.003})_{\Sigma 0.99}\,O_2$ from the Greenbushes granitic pegmatite, Western Australia, contains lamellae (~5 × 50 μm in size) of disordered ferrocolumbite $(Fe^{2+}_{0.80}\,Mn^{2+}_{0.12}\,Ti^{4+}_{0.07})_{\Sigma 0.99}\,(Nb^{5+}_{1.48}\,Ta^{5+}_{0.28}\,Ti^{4+}_{0.13}\,W^{6+}_{0.09}\,Sn^{4+}_{0.01})_{\Sigma 1.99}\,O_6$. The lamellae apparently formed by exsolution from the original rutile-like phase, which is supported by several features, most notably by the fixed structural orientation of lamellae with respect to the host phase. Single-crystal X-ray diffraction shows that ferrocolumbite lamellae are present in four orientations, with the reciprocal axis $\mathbf{c_{fcl}}^*$ of each approximately parallel to one of the rutile directions $[101]^*$, $[011]^*$, $[\bar{1}01]^*$, $[0\bar{1}1]^*$. The ferrocolumbite $\mathbf{a}^*$ axes are strictly parallel to the $\pm\mathbf{a_1}^*$ and $\pm\mathbf{a_2}^*$ axes of rutile, whereas $\mathbf{b_{fcl}}^*$ is not parallel to any rational reciprocal direction of rutile. This may be the first documented case where the mutual crystallographic orientation between host rutile and a precipitate of disordered ferrocolumbite has been determined. Weak reflections corresponding to a ferrocolumbite supercell with a triple *a* indicate the presence of ordered ferrocolumbite in what appears to be a parallel orientation with the disordered ferrocolumbite.

Keywords: rutile, ferrocolumbite, ixiolite, exsolution process, optimal phase-boundary, granitic pegmatite, Greenbushes, Australia.

SOMMAIRE

Un échantillon de rutile niobifère $(Ti^{4+}_{0.63}\,Nb^{5+}_{0.14}\,Fe^{2+}_{0.11}\,Ta^{5+}_{0.08}\,Fe^{3+}_{0.02}\,W^{6+}_{0.01}\,Sn^{4+}_{0.003})_{\Sigma 0.99}\,O_2$ provenant de la pegmatite granitique de Greenbushes, en Australie occidentale, contient des lamelles ~5 × 50 μm de ferrocolumbite désordonnée $(Fe^{2+}_{0.80}\,Mn^{2+}_{0.12}\,Ti^{4+}_{0.07})_{\Sigma 0.99}\,(Nb^{5+}_{1.48}\,Ta^{5+}_{0.28}\,Ti^{4+}_{0.13}\,W^{6+}_{0.09}\,Sn^{4+}_{0.01})_{\Sigma 1.99}\,O_6$. Les lamelles se seraient formées par exsolution à partir d'un minéral ayant les propriétés du rutile, hypothèse qu'étayent plusieurs propriétés, dont la présence d'une orientation structurale fixe des lamelles par rapport à la phase hôte. La diffraction X sur monocristaux montre que les lamelles de ferrocolumbite sont développées en quatre orientations, avec l'axe réciproque $\mathbf{c_{fcl}}^*$ de chacun à peu près parallèle à une des directions du rutile, $[101]^*$, $[011]^*$, $[\bar{1}01]^*$, $[0\bar{1}1]^*$. L'axe $\mathbf{a}^*$ des quatre domaines de la ferrocolumbite est strictement parallèle à $\pm\mathbf{a_1}^*$ et $\pm\mathbf{a_2}^*$ du rutile, tandis que $\mathbf{b_{fcl}}^*$ n'est parallèle à aucune direction réciproque du rutile. Notre exemple pourrait bien s'avérer la première documentation de l'orientation cristallographique mutuelle entre un rutile hôte et un précipité de ferrocolumbite désordonné. De faibles réflexions correspondant à une supermaille de ferrocolumbite ayant un paramètre *a* triplé indiquent la présence d'une ferrocolumbite ordonnée dans ce qui semble être une orientation parallèle avec la ferrocolumbite désordonnée.

(Traduit par la Rédaction)

Mots-clés: rutile, ferrocolumbite, ixiolite, processus d'exsolution, interface optimale, pegmatite granitique, Greenbushes, Australie.

INTRODUCTION

Presently, in the industrial world, there is a growing demand for niobium and tantalum. Both are processed from tantaloniobates (oxide minerals of Nb and Ta) that occur either as individual grains or as inclusions in host minerals such as rutile or cassiterite. Tantaloniobates such as ixiolite and columbite have commonly been described in the literature as inclusions or as precipitates (*i.e.*, products of exsolution) in rutile (Černý *et al.* 1964, 1981, 1989, 1999, 2000). However, these studies relied on reflected-light microscopy, electron-micro-

---

[§] *Present address*: Institute of Inorganic Chemistry, Academy of Sciences of the Czech Republic, CZ–250 68 Řež u Prahy, Czech Republic. *E-mail address*: klemari@iic.cas.cz

[¶] *Present address*: Institute of Materials Chemistry, Technical University of Ostrava, CZ–708 33 Ostrava–Poruba, Czech Republic. *E-mail address*: rieder@cesnet.cz

probe analyses, and X-ray powder diffraction, which do not suffice to differentiate unequivocally between inclusions *sensu stricto* and exsolution products.

We focus here on an occurrence of niobian rutile from the Greenbushes granite pegmatite, in Western Australia. The pegmatite is an important producer of Nb and Ta, and the heavy-mineral concentrate also contains grains of niobian rutile. Here, we used X-ray diffraction (precession method) and electron-microprobe analysis to characterize a grain of niobian rutile. The observations are used to propose a likely sequence that led to the formation of the rutile–ferrocolumbite intergrowth.

The Geological Context

The rutile grain described in this paper was found in a heavy-mineral concentrate from the granitic pegmatite deposit at Greenbushes, Western Australia. The pegmatite at Greenbushes falls into the class of rare-metal pegmatites as defined by Černý (1991), which represent an important source of Sn, Ta and Li.

The Greenbushes mineral field is located about 250 km south of Perth, in the southwestern Yilgarn block, within the Western Gneiss terrane. The intrusive rocks in the Greenbushes pegmatite district are concentrated

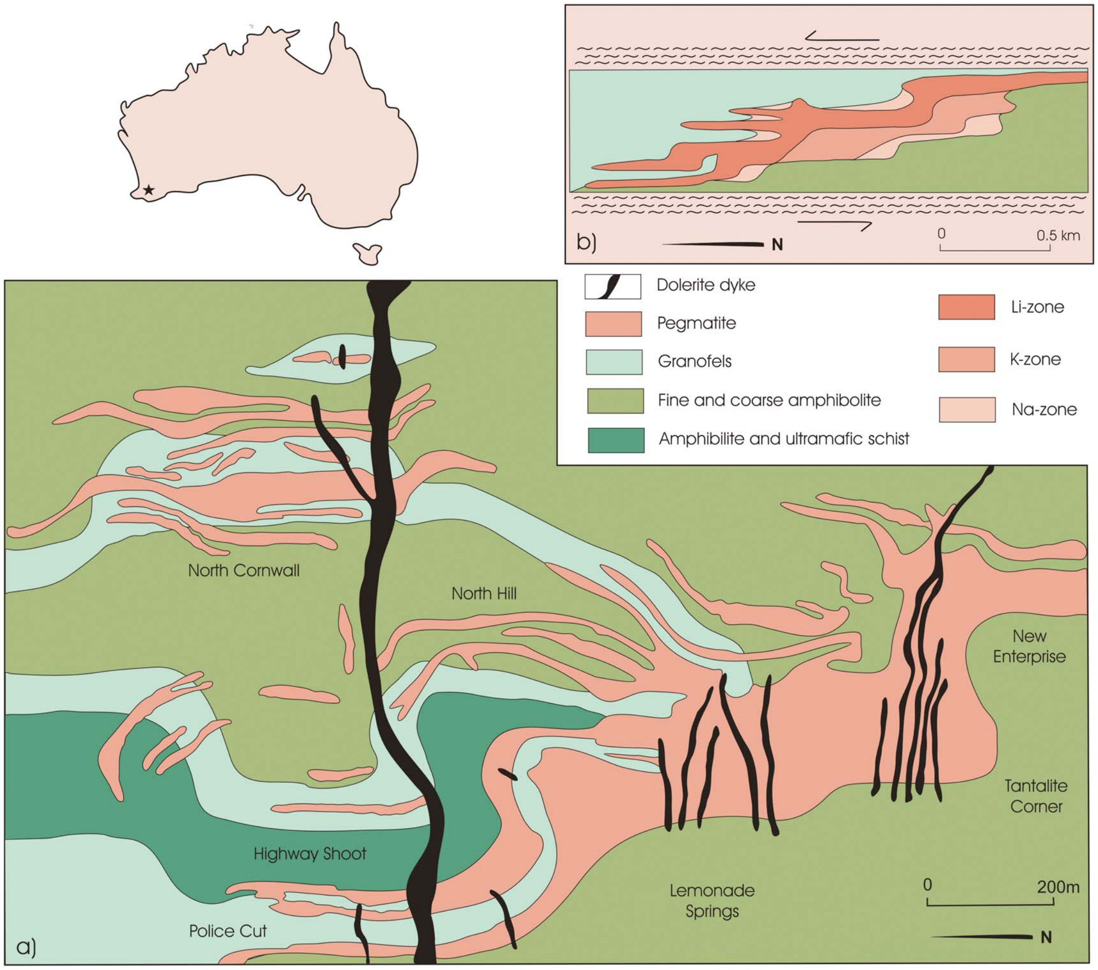

FIG. 1. Geology of the Greenbushes pegmatite deposit: a) geological map, b) schematic model of the intrusion of the pegmatite during progressive shearing (after Bettenay *et al.* 1998).

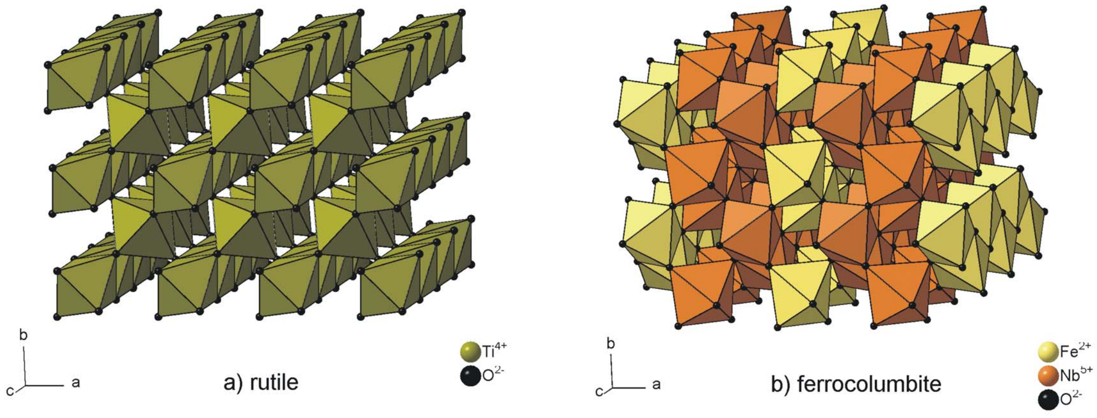

a) rutile

b) ferrocolumbite

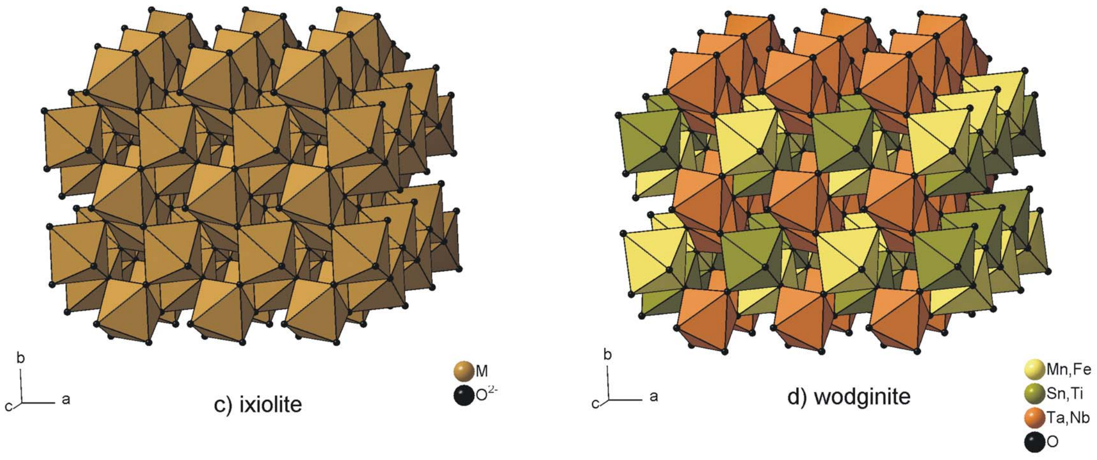

c) ixiolite

d) wodginite

FIG. 2. Structures of a) rutile, b) ixiolite, c) ferrocolumbite, and d) wodginite.

along an ancient regional shear-zone, analogous to the present-day San Andreas Fault system. The pegmatite was emplaced along the contact of mafic amphibolites, ultramafic rocks, and laminated metasedimentary rocks (Figs. 1a, b). The estimated conditions during the emplacement are 550–625°C and 4–5 kbars (Partington 1990). The pegmatite displays the same shear fabric as its host rocks and shows evidence of syntectonic crystallization. The age of the pegmatite was determined by U–Pb dating of zircon as 2.53 Ga (Solomon & Groves 1994).

The body of the pegmatite is 3000 m long, 40–250 m wide and reaches a depth of 400 meters. The pegmatite and its surrounding rocks were strongly tectonized and underwent metamorphic recrystallization. Nevertheless, the deformation is concentrated along the contacts, and therefore the zoning of the inner pegmatite remains well preserved. Close to the contact, a K-enriched zone is developed, whereas toward the center, a Na-enriched zone prevails. Both of these zones are enveloped by a Li-enriched zone. Mineralization, represented mainly by cassiterite and minerals of the columbite–tantalite group, is concentrated in the Na-enriched zone (Fig. 1b).

STRUCTURAL BACKGROUND

The structures of all species involved in this investigation, *i.e.*, rutile, ferrocolumbite, and ixiolite, are analogous. They all are based on hexagonal close-packing of oxygen atoms and octahedrally coordinated cations, but the octahedra have different arrangements in space.

Rutile is tetragonal, space group $P4_2/mnm$. The cell parameters of synthetic TiO_2 are: $a = b$ 4.593, c 2.957 Å (Seki *et al.* 1984). Its structure consists of edge-sharing TiO_6 octahedra that form chains along the **c** axis and are interconnected in the [110] direction by interconnected apices of octahedra (Fig. 2a).

Members of columbite–tantalite group (Fe,Mn)(Nb,Ta)$_2$O$_6$ are orthorhombic, space group *Pbcn*, with cell parameters *a* 14.26, *b* 5.732, *c* 5.038 Å (Weitzel 1976). Where ordered, the structure consists of alternating sheets of (Fe,Mn)-bearing octahedra and (Nb,Ta)-bearing octahedra (in a 1:2 ratio), as indicated in Figure 2b. The sheets are perpendicular to the **a** axis and consist of zig-zag chains of octahedra arranged parallel to the **c** axis. In the disordered form, the *a* parameter is reduced to 1/3, and the structure becomes essentially identical with that of ixiolite.

Ixiolite is a mixed oxide of Ta, Nb, Fe, Mn and Sn with the formula (Ta,Fe,Sn,Nb,Mn)$_4$O$_8$. Significant quantities of Ti and W may also be present. Ixiolite is orthorhombic, space group *Pbcn*, with unit-cell parameters *a* 4.742, *b* 5.731, *c* 5.152 Å (Nickel *et al.* 1963). Cation–oxygen octahedra form a three-dimensional framework (Fig. 2c) identical to that of disordered columbite. However, by cation ordering, ixiolite loses its orthorhombic symmetry and becomes a monoclinic member of wodginite group (Mn,Fe)(Sn,Ti)(Ta,Nb)$_2$O$_8$ (Fig. 2d). According to Černý *et al.* (1998), the reason for such a distortion may be elevated contents of Sn or Ti as well as the prevalence of Ta over Nb and of Mn over Fe in ixiolite compared to levels in the columbite–tantalite group.

MICROSCOPY AND CHEMICAL COMPOSITION

In reflected light under a microscope, the rutile in our sample (light grey) contains dark grey lamellae (~5 × 50 μm in size) that are needle-like in shape and occur in parallel sets; three such sets can be seen in Figure 3. Their needle-like shape indicates a high strain at the interface between the lamellae and the rutile matrix at the nucleation stage (Palmer *et al.* 1988). In order to reduce maximum strain that occurs in the junctions, right-angled domain walls become curved, and later two of them combine to form a needle-like precipitate. The surface energy is further reduced by migration of the "needle" into the matrix. This phenomenon was first described in twin lamellae in leucite by Palmer *et al.* (1988).

Chemical analyses were performed on a CamScan 4 electron microprobe in energy-dispersion mode at 20 kV, with a specimen current of 3 nA. The following standards were used: rutile TiO$_2$ (Ti), cassiterite SnO$_2$ (Sn), columbite FeNb$_2$O$_6$ (Nb), tantalite Fe(Ta,Nb)$_2$O$_6$ (Ta), fayalite Fe$_2$SiO$_4$ (Fe), Mn$_2$SiO$_4$ (Mn), and scheelite CaWO$_4$ (Ca,W). The formulas were calculated on the assumption of 24 atoms of oxygen and 12 cations per unit cell. This facilitates a direct comparison of cation quantities and proportions in all minerals that have to be considered (rutile, ferrocolumbite, ixiolite and wodginite). The content of Fe$_2$O$_3$ was calculated to prevent cation surplus over 12 atoms per formula unit (*apfu*).

Results of nine analyses of the host rutile and the lamellae are shown in Table 1. The composition of this sample of rutile is highly enriched in Nb (≤19.01 wt.% Nb$_2$O$_5$), Ta (≤19.35 wt.% Ta$_2$O$_5$), and Fe (≤8.29 wt. % FeO). In addition, rutile also contains significant amounts of Fe^{3+} (≤2.07 wt.% Fe$_2$O$_3$), W (≤2.60 wt.% WO$_3$) and traces of Sn (≤0.66 wt.% SnO$_2$). The chemical composition of the lamellae is very close to that of ferrocolumbite, ideally FeNb$_2$O$_6$; Nb (≤54.41 wt.% Nb$_2$O$_5$) strongly dominates over Ta (≤16.88 wt.% Ta$_2$O$_5$), and Fe (≤16.07 wt.% FeO) prevails over Mn (≤2.85 wt.% MnO). In addition to the main elements, the lamellae are rich in W (≤7.48 wt.% WO$_3$) and Ti (≤4.62 wt.% TiO$_2$). Small amounts of Fe^{3+} (≤0.52 wt.% Fe$_2$O$_3$) and Sn (≤0.35 wt.% SnO$_2$) also were detected.

In both phases, extensive chemical substitutions evidently occur. Beside the common homovalent substitutions of Ti^{4+} by Sn^{4+}, Fe^{2+} by Mn^{2+}, and Nb^{5+} by Ta^{5+}, the following heterovalent mechanisms may be involved: 1) 2 Ti^{4+} ↔ Fe^{3+} + (Nb,Ta)$^{5+}$, 2) 3 Ti^{4+} ↔ (Fe,Mn)$^{2+}$ + 2 (Nb,Ta)$^{5+}$, 3) 2 Ti^{4+} ↔ W^{6+} + (Fe,Mn)$^{2+}$, and 4) 2 (Nb,Ta)$^{5+}$ ↔ W^{6+} + (Sn,Ti)$^{4+}$.

The above mechanisms of substitution were distinguished by successive subtraction of unique elements from the bulk composition until a pure rutile composition was obtained (a similar procedure is used to resolve garnet end-members). Substitutions considered during the calculation had previously been described in the literature (Neiva 1996, Černý *et al.* 1998, 2000). The ferrocolumbite lamellae concentrate Fe^{2+}, Mn^{2+}, Nb^{5+} and W^{6+}, whereas the niobian rutile prefers Fe^{3+} and Ta^{5+}. Otherwise, both phases have a composition that is essentially homogeneous. No diffusion gradients within the matrix were observed.

In terms of the columbite quadrilateral (Fig. 4), the composition of the rutile host is restricted to the Mn-poor section of the diagram, whereas the ferrocolumbite lamellae show enrichment in Mn. In contrast, the relative Ta content is higher in the host than in the lamellae. In the (Ti + Sn + W) – (Fe + Mn) – (Nb + Ta) triangle (Fig. 5), the points representing the chemical composition of the rutile host and the ferrocolumbite lamellae plot on a line that connects the Ti apex of the triangle with the stoichiometric composition of pure columbite–tantalite (Fe,Mn)(Nb,Ta)$_2$O$_6$ on the opposite side of the triangle. According to the volume ratio of the rutile host to the ferrocolumbite lamellae (~3:1), the bulk composition of the primary phase can be estimated as (at.%): (Ti + Sn)$_{0.52}$(Nb + Ta)$_{0.30}$(Fe + Mn)$_{0.18}$, which corresponds to 48% (Fe,Mn)(Nb,Ta)$_2$O$_6$. Černý *et al.* (2000) reported 34–38% (Fe,Mn)(Nb,Ta)$_2$O$_6$ in the primary phase for a similar case.

SINGLE-CRYSTAL X-RAY DIFFRACTION

Inasmuch as it appears that the mutual crystallographic orientation of lamellae and the host may be important in deducing the cooling history of the primary

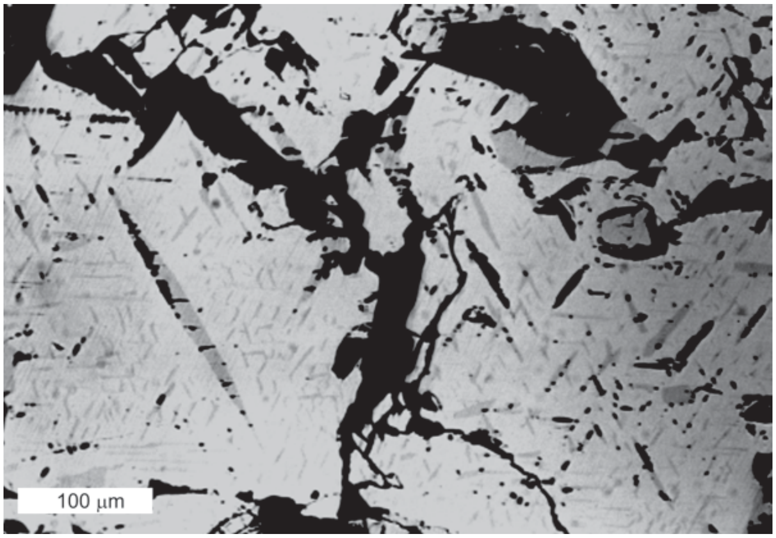

FIG. 3. Dark grey lamellae of ferrocolumbite (~5 × 50 mm in size) in light grey rutile (black areas are holes in the sample). The two scales of coarseness may reflect two episodes of exsolution. Polished section in reflected light.

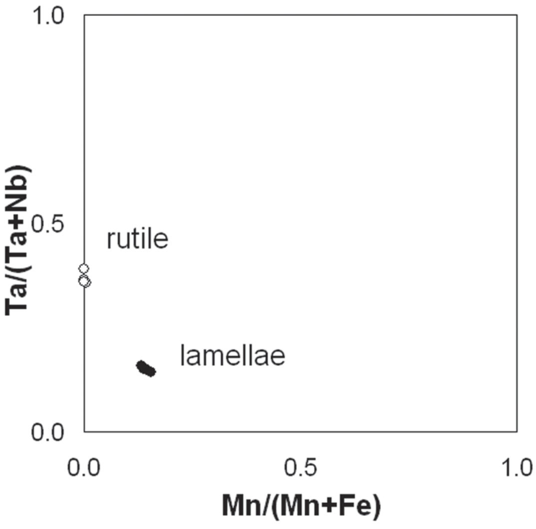

FIG. 4. Chemical composition of the rutile host (open circles) and the ferrocolumbite lamellae (solid circles) plotted in the columbite–tantalite quadrilateral (atom fractions).

TABLE 1. CHEMICAL COMPOSITIONS OF RUTILE HOST AND FERROCOLUMBITE LAMELLAE IN NIOBIAN RUTILE FROM THE GREENSBUSHES GRANITIC PEGMATITE, AUSTRALIA

	fcl	fcl	fcl	fcl	fcl	rt	rt	rt	rt
Fe_2O_3 wt.%	0.00	0.00	0.00	0.00	0.52	1.25	1.86	2.07	1.91
FeO	16.07	16.05	15.44	15.79	15.63	8.29	7.85	7.32	7.23
MnO	2.63	2.40	2.61	2.49	2.85	0.00	0.00	0.04	0.00
TiO_2	4.26	4.30	4.43	4.62	4.54	50.65	50.74	51.50	51.65
CaO	0.00	0.02	0.13	0.07	0.08	0.00	0.00	0.01	0.00
SnO_2	0.12	0.35	0.11	0.09	0.20	0.22	0.39	0.37	0.66
Ta_2O_5	15.59	16.88	15.49	15.55	15.11	19.35	17.73	17.56	17.23
WO_3	6.68	5.73	5.76	6.90	7.48	2.60	2.47	2.04	2.16
Nb_2O_5	53.20	54.41	53.25	52.86	53.99	18.12	18.66	19.01	18.52
Sb_2O_3	0.00	0.00	0.00	0.00	0.00	0.00	0.00	0.00	0.00
Na_2O	0.07	0.00	0.00	0.04	0.15	0.00	0.00	0.09	0.11
Total	98.62	100.14	97.22	98.41	100.54	100.48	99.70	100.02	99.48
Fe^{3+} *apfu*	0.000	0.000	0.000	0.000	0.094	0.187	0.280	0.309	0.286
Fe^{2+}	3.286	3.233	3.188	3.230	3.124	1.382	1.309	1.211	1.201
Mn^{2+}	0.545	0.490	0.546	0.516	0.576	0.000	0.000	0.007	0.000
Ti^{4+}	0.784	0.779	0.823	0.850	0.816	7.597	7.610	7.660	7.714
Ca^{2+}	0.000	0.005	0.034	0.018	0.021	0.000	0.000	0.002	0.000
Sn^{4+}	0.012	0.034	0.011	0.009	0.019	0.018	0.031	0.029	0.053
Ta^{5+}	1.037	1.106	1.040	1.034	0.982	1.049	0.961	0.944	0.930
W^{6+}	0.423	0.358	0.369	0.437	0.464	0.134	0.127	0.105	0.111
Nb^{5+}	5.880	5.924	5.944	5.845	5.835	1.633	1.682	1.699	1.663
Sb^{3+}	0.000	0.000	0.000	0.000	0.000	0.000	0.000	0.000	0.000
Na^+	0.033	0.000	0.000	0.019	0.070	0.000	0.000	0.035	0.043
Total	11.999	11.927	11.954	11.958	12.000	12.000	12.000	12.000	12.000
Mn/(Mn+Fe)	0.142	0.132	0.146	0.138	0.156	0.000	0.000	0.006	0.000
Ta/(Ta+Nb)	0.150	0.157	0.149	0.150	0.144	0.391	0.364	0.357	0.359

The proportion of Fe_2O_3 was calculated to prevent cation surplus over 12.000 *apfu*. The structural formulae were calculated on the basis of 24 atoms of oxygen per formula unit.

high-temperature phase, we took a series of precession photographs (Enraf–Nonius camera). Mostly, unfiltered Mo$K\alpha$ radiation was used in order to maintain sufficient intensity. For some photographs, in which continuous radiation hampered the interpretation, Zr-filtered radiation was used.

First, we measured the unit-cell parameters of the niobian rutile host ($a = b$ 4.642, c 2.998 Å) and of the phase in lamellae (a 4.642, b 5.714, c 5.033 Å). The latter unit-cell corresponds to that of ixiolite or disordered ferrocolumbite; the chemical data tip the balance in favor of disordered ferrocolumbite. If the phase were ixiolite, cation ratios would have to conform to the formula of the wodginite group (the ordered counterpart of ixiolite), but they do not.

In addition to reflections of rutile, all photographs contain weak reflections of ferrocolumbite. The 0*kl* (= *h*0*l*) net of rutile is relatively straightforward to interpret (Fig. 6). The crystallographic orientation of ferrocolumbite with respect to rutile is such that the 0*kl* reciprocal net of ferrocolumbite overlaps with the 0*kl* reciprocal net of rutile. Diffraction spots $\overline{0}11_{\mathrm{rt}}$ and 021_{fcl} lie close to each other and so do spots $0\overline{1}1_{\mathrm{rt}}$ and 002_{fcl}. The $\mathbf{a}_{\mathrm{fcl}}$* direction is parallel to $\mathbf{a}^*_{\mathrm{rt}}$, and the $\mathbf{b}_{\mathrm{fcl}}$* direction is not parallel to any rational reciprocal direction of rutile. However, the photographs are somewhat more complicated because there are three additional orientations of ferrocolumbite, which arise because of the tetragonal symmetry of rutile. The **c*** directions of fcl_1 and

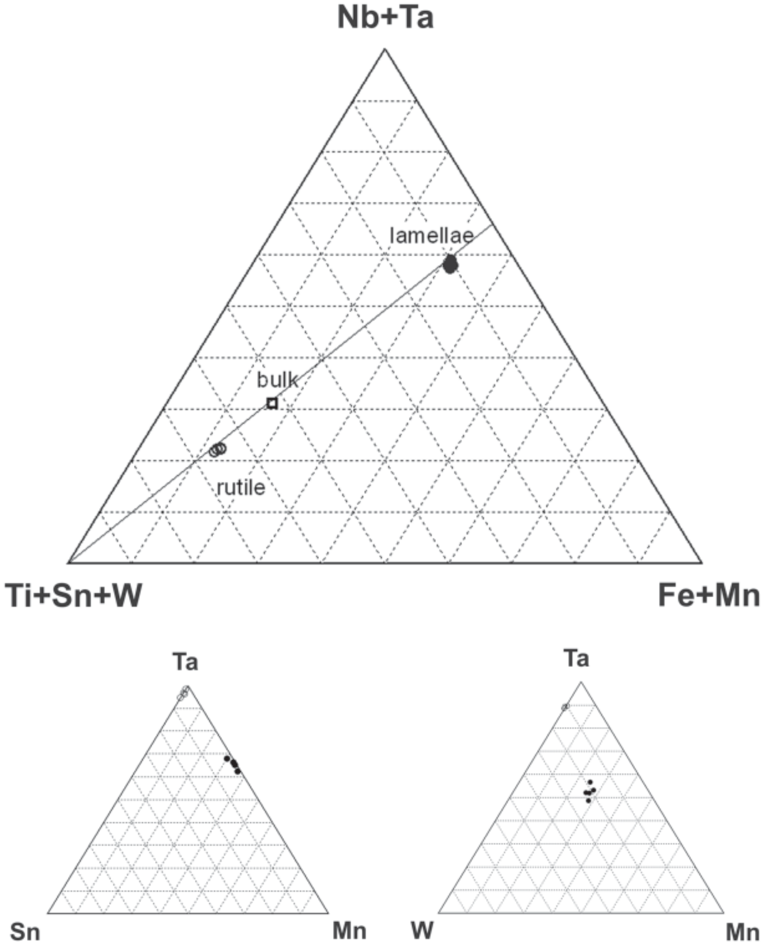

FIG. 5. Chemical composition of the rutile host (open circles), the ferrocolumbite lamellae (solid circles) and the bulk composition of the primary phase (open square) plotted in the triangle (Ti + Sn + W) – (Fe + Mn) – (Nb + Ta); in atom percent. Theoretically, columbite–tantalite plots at one-third of the distance between apices Nb + Ta and Fe + Mn.

fcl$_2$ are visible on the photograph, being approximately parallel to [0$\bar{1}\bar{1}$]* and [011]* of rutile, respectively. The corresponding **a*** directions of columbite (fcl$_1$ and fcl$_2$) coincide with **a*** and **–a*** of rutile, which are normal to the page. The **a*** directions of fcl$_3$ and fcl$_4$ are parallel to **b*** and **–b*** of rutile, and their **c*** directions are located in the *h*01 reciprocal net of rutile, which is normal to the page.

The interpretation of the *hk*0 net of rutile (Fig. 6) is somewhat trickier because strong reflections of rutile are flanked by satellite spots that belong to the *h*2*kk* net(s) of ferrocolumbite (221 of two ferrocolumbite orientations flank 220 of rutile). The *h*2*kk* net is not strictly

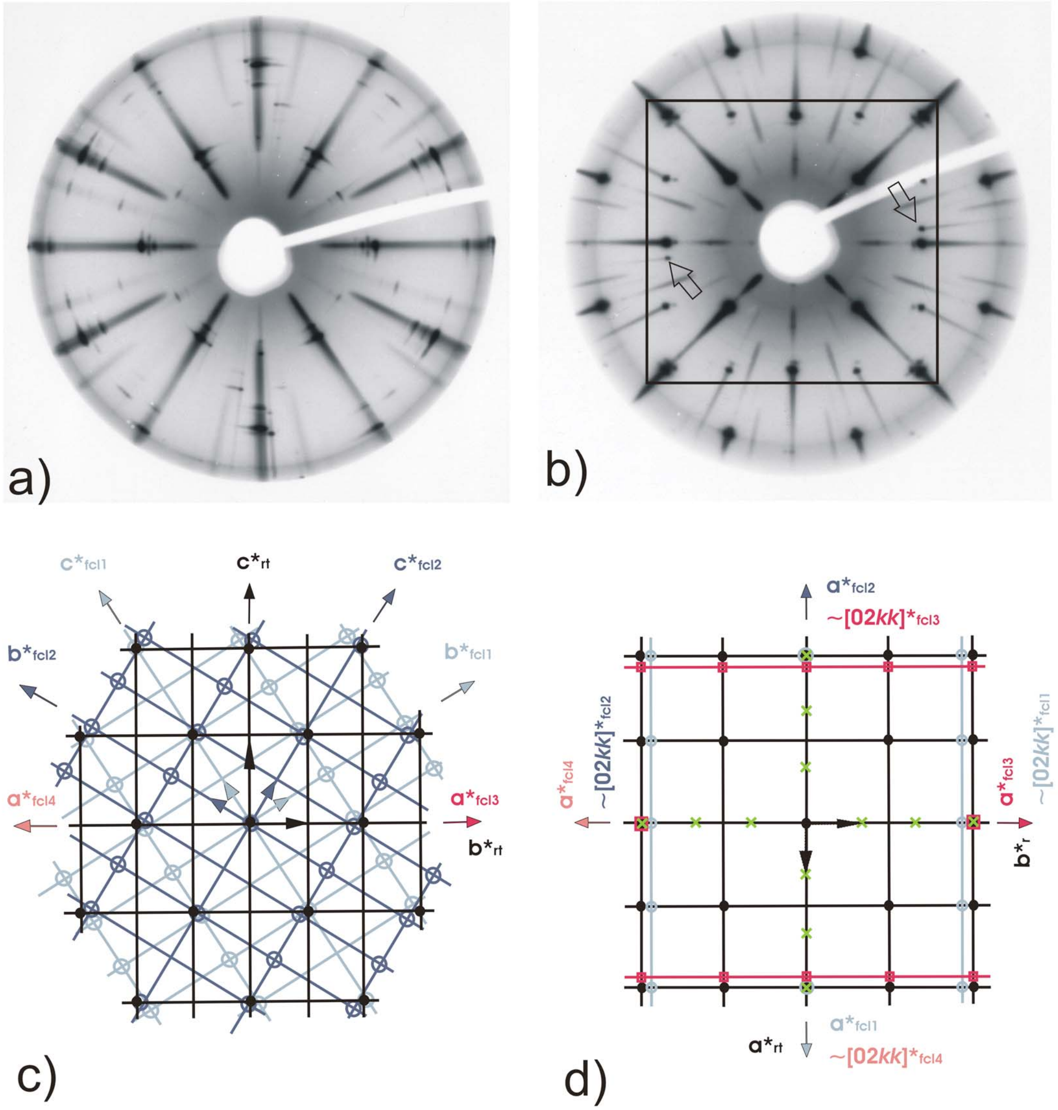

FIG. 6. Precession photographs of rutile with ferrocolumbite lamellae: a) looking down [100]* of rutile, b) looking down [001]* of rutile. The ferrocolumbite lamellae follow all planes of {101} of rutile, and the reciprocal axis $\mathbf{c}_{\mathbf{fcl}}$* of each precipitate of ferrocolumbite is approximately parallel to one of the rutile directions [101]*, [011]*, [$\bar{1}$01]*, [0$\bar{1}$1]*; a) unfiltered Mo*K*α radiation, c) interpretation. The $\mathbf{a}_{\mathbf{fcl}}$* axis of ferrocolumbite is parallel to the $\mathbf{a}_{\mathbf{rt}}$* axis of rutile; b) Zr-filtered Mo*K*α radiation, d) interpretation. The direction of axis $\mathbf{b}_{\mathbf{fcl}}$* is not parallel to any rational reciprocal direction of rutile. Symbols: ● rutile, ○ ferrocolumbite 1 and 2, □ ferrocolumbite 3 and × ordered ferrocolumbite. Relatively strong reflections close to 020 and 0$\bar{2}$0 of rutile belong to a randomly oriented additional crystal.

parallel to the *hk*0 net of rutile, but it is so close that it cannot be screened away. On an overexposed Zr-filtered photograph (Fig. 6b) taken with an intensifier foil, there are also weak reflections present corresponding to a supercell whose *a* is three times larger than that of the disordered ferrocolumbite and that appear to be in a perfectly parallel orientation with it. These reflections indicate the presence of yet another phase, ordered ferrocolumbite. Diffraction spots of disordered ferrocolumbite are somewhat irregular in shape and slightly arcuate, but those from the ordered phase appear sharper. One would expect to observe this arrangement if there were two stages of unmixing (at two different temperatures?) or unmixing followed by an incipient ordering of cations in the unmixed lamellae. The intensities of the additional reflections of the ordered ferrocolumbite phase are considerably weaker than those of the disordered ferrocolumbite, which means that in terms of volume, the disordered phase strongly prevails. It is difficult to predict whether the ordered phase can at all be identified under the electron microprobe because the composition of both variants of ferrocolumbite may differ very little if at all.

Another feature visible in overexposed photographs is the appearance of faint Debye–Scherrer rings running through the strongest reflections of ferrocolumbite. Thus a small part of the ferrocolumbite is polycrystalline, and may correspond to ferrocolumbite inclusions *sensu stricto* captured during the growth of rutile.

OPTIMAL PHASE-BOUNDARIES

Calculation of the optimal phase-boundaries allows us to estimate the orientation of the actual interface between two phases in an overgrowth, which cannot be determined by interpreting precession photographs. In general, the composition plane along which the host phase is in contact with the lamellae is not crystallographically rational like in crystal morphology, but irrational, and its orientation is dictated by a strive to attain a two-dimensional match along the interface.

Careful measurements of coordinates of diffraction spots 011 and $0\bar{1}1$ of rutile and 021 and 002 of ferrocolumbite (fcl_1 in Fig. 6b) in the precession photographs permitted us to define analogous subcells for both phases that were input into the DIMFIT program (written by M.E. Fleet), which calculates optimal phase-boundaries according to the approach of Robinson *et al.* (1977). The calculation yields two solutions (Table 2); in order to decide which one corresponds to the overgrowth at hand, one has to either determine the orientation of the composition plane with respect to crystallographic directions of one of the phases or measure the reciprocal-lattice rotation. Owing to the scarcity of the material available, we could not make sections to measure the orientation of the composition plane in direct space, but the reciprocal-lattice rotation observed in precession photographs is in good agreement with one of the calculated solutions (Table 2).

As already mentioned, the intensities of additional reflections due to the ordered ferrocolumbite phase are much weaker than those of the disordered ferrocolumbite. In addition, all the other reflection spots of the ordered phase are lost owing to coincidence with stronger reflections of the disordered phase. Therefore, it is impossible to obtain data that would permit a calculation of the optimal phase-boundary for the ordered ferrocolumbite.

DISCUSSION

All data available are in agreement with the hypothesis that the ferrocolumbite–rutile intergrowth studied as a low-temperature (and low-pressure) breakdown of an originally homogeneous primary phase. However, no concentration gradient in the matrix was observed, which indicates that the process effectively went to completion. The two phases now are in a late stage of the exsolution process, characterized by coarsened lamellae and lost coherency along their interface.

At this point, a few additional comments are in order on the character of the primary phase, and on the transformation mechanism. As we do not have any data that would allow us to identify the primary phase directly, we can only make inferences by comparing our results with data found in literature.

The primary phase

The chemical composition of the primary phase can be estimated from the chemical composition of the products of exsolution and their volumetric proportions according to the lever rule. The calculation shows about 48 mol.% $(\mathrm{Fe,Mn})(\mathrm{Nb,Ta})_2\mathrm{O}_6$ in TiO_2. Regarding the structure, there are two candidates, the rutile structure

TABLE 2. RESULTS OF THE OPTIMAL PHASE-BOUNDARY CALCULATION FOR THE EXSOLUTION-RELATED PAIR RUTILE – FERROCOLUMBITE

lattice rotations	$[011]^*_{\mathrm{rt}} \wedge [021]^*_{\mathrm{fcl}}$	$[0\bar{1}1]^*_{\mathrm{rt}} \wedge [002]^*_{\mathrm{fcl}}$	
solution I (calculated)	0.38°	5.67°	
solution II (calculated)	5.30°	0.01°	
measured	~5.50°	~0.00°	
	angle of c_{rt} with composition plane	angle of c_{fcl} with composition plane	$c_{\mathrm{rt}} \wedge c_{\mathrm{fcl}}$
solution I (calculated)	30.39°	3.20°	27.18°
solution II (calculated)	38.49°	71.36°	32.86°
hypothetical: $\{011\}_{\mathrm{rt}} \parallel \{001\}_{\mathrm{fcl}}$	57.14°	90.00°	32.86°
measured	n.m.	n.m.	32.86°

n.m.: not measured.

and the ixiolite structure (also referred to as disordered columbite, TiO_2-II or α-PbO_2 structure).

The presence of the rutile structure as a high-temperature phase in similar systems was reported by Wenger & Armbruster (1993), and Baumgarte & Blachnik (1994). Wenger & Armbruster (1993) synthesized phases in the system $NiNb_2O_6$ – TiO_2. At lower temperature, $NiNb_2O_6$ has a columbite structure and is separated from rutile by a miscibility gap. Above 1400°C, the miscibility gap closes and only a solid solution with the rutile structure is present. Baumgarte & Blachnik (1994) searched for electro-optical materials with a composition $M^{2+}M^{4+}Nb_2O_8$, which has a stoichiometry similar to wodginite ($MnSnTa_2O_8$). Among the cations studied are Ti^{4+}, Mg^{2+}, Mn^{2+}, Co^{2+}, Ni^{2+}, Cu^{2+}, and Zn^{2+}. The syntheses were carried out at 1200°C. The rutile structure was observed for all the above cations except for Mn^{2+}, for which a mixture of TiO_2 with a compound of the ixiolite structure was obtained. That could happen if the temperature of synthesis is below the crest of the solvus. Furthermore, a synthetic $FeNb_2O_6$ (synthesized at 850°C) was reported to have a rutile structure by Aruga *et al.* (1985).

Titanian ixiolite was suggested by Černý *et al.* (1989) as a likely homogeneous orthorhombic precursor for a similar mineral association, even though no direct proof was presented. Nevertheless, the ixiolite structure should still be considered as a candidate. First, it is a very flexible structure. From natural samples, we know that it can accommodate a wide range of chemical compositions (Černý *et al.* 1998), and it orders to either the columbite or wodginite structure depending on its chemical composition. Second, the ixiolite structure can also be adopted by TiO_2 under conditions of high pressure, *ca.* 10 GPa (Bendeliani *et al.* 1966, Kusaba *et al.* 1988, Sato *et al.* 1991, Swamy *et al.* 2001, Sasaki 2002, Withers *et al.* 2003). In this case, it is referred to as the α-PbO_2 structure or TiO_2-II. Urusov *et al.* (1996) observed a transformation of twinned rutile to a metastable α-PbO_2 phase during non-hydrostatic compression.

To sum up, we believe that our assemblage of rutile + disordered ferrocolumbite is best modeled by the synthetic system TiO_2 – $NiNb_2O_6$ of Baumgarte & Blachnik (1994). Moreover, a high- temperature rutile-like phase of $FeNb_2O_6$ was reported by Aruga *et al.* (1985). Last but not least, a metastable low-temperature polymorph of TiO_2, brookite, has an ixiolite-like structure (Meagher & Lager 1979), which also supports the fact that at higher temperatures, the rutile structure is stable relative to the ixiolite structure. Therefore, considering that the pressure needed to obtain the α-PbO_2 phase is quite high (several GPa), we conclude that the primary phase most likely had the rutile structure. This prediction also complies with a general rule about lowering the symmetry during a phase transformation in going from higher to lower temperatures.

The mechanism of transformation

The rutile and columbite structures have interesting analogies. The columbite structure can be obtained from that of rutile by displacing every other cation of a chain running in the **c** direction to the nearest octahedral void in the neighboring layer of cations, as described by Baumgarte & Blachnik (1994) and shown on Figure 7a. This mechanism seems simple and energetically favorable. However, it leads to the relationship $\mathbf{c}_{rt} \perp \mathbf{c}_{fcl}$, which does not correspond to our observations. Another mechanism was proposed by Urusov *et al.* (1996); they considered the (011) twin planes in rutile as nuclei for further growth of the α-PbO_2 phase (Fig. 7b). The twinning is initiated by non-hydrostatic compression and shearing in the sample. In this case, the mutual structural orientation $\mathbf{c}_{fcl} \perp (011)_{rt}$ is in agreement with our results. Nevertheless, we have not observed any twinning in rutile, which could be attributed to the fact that all twins representing the other twin orientation were transformed into ferrocolumbite. The ixiolite structure can be further stabilized by either high pressure (Bendeliani *et al.* 1966, Kusaba *et al.* 1988, Sato *et al.* 1991, Swamy *et al.* 2001, Sasaki 2002, Withers *et al.* 2003) or a large difference between the radius of the cations (Baumgarte & Blachnik 1994).

Structural planes parallel to the interface observed by Urusov *et al.* (1996) are shown on Figure 8. Sheets of octahedra parallel to (011) of rutile and (001) of disordered ferrocolumbite are illustrated. One can clearly see that the main pattern of corner-sharing octahedra that point alternatively in opposite directions remains the same in the two structures. The network only becomes a bit more homogeneous and straightened up in the orthorhombic structure. Furthermore, there is also a very good agreement in distances normal to these crystallographic planes, $d(011)_{rt} = 2.518$ Å and $d(002)_{fcl} = 2.516$ Å. On the contrary, dimensions of $[011]_{rt}$ and $[001]_{fcl}$ are quite different, $[011]_{rt} = 5.526$ Å, $[001]_{fcl} = 5.714$ Å.

From the precession photographs, we were able to determine the mutual orientation between rutile and ferrocolumbite lattices, which corresponds to roughly 30° between the **c** directions of rutile and ferrocolumbite. However, we were not able to measure the actual crystallographic orientation of the interface in a thin section. Instead, we used the calculations of the optimal phase-boundaries to determine the interface orientation (Table 2). A large difference in the orientation of the interface in comparison to the orientation of the expected plane $(011)_{rt}$ with respect to the **c** direction of rutile was observed. This difference, as well as the difference in dimensions mentioned above, can be attributed to the advanced stage of the exsolution process. The calculated angular relations correspond to input values of unit-cell parameters. To the extent that the current unit-cell data differ from those at the time of nucleation, the measurements will not equal the predictions perfectly. Indeed, the lamellae in the present over-

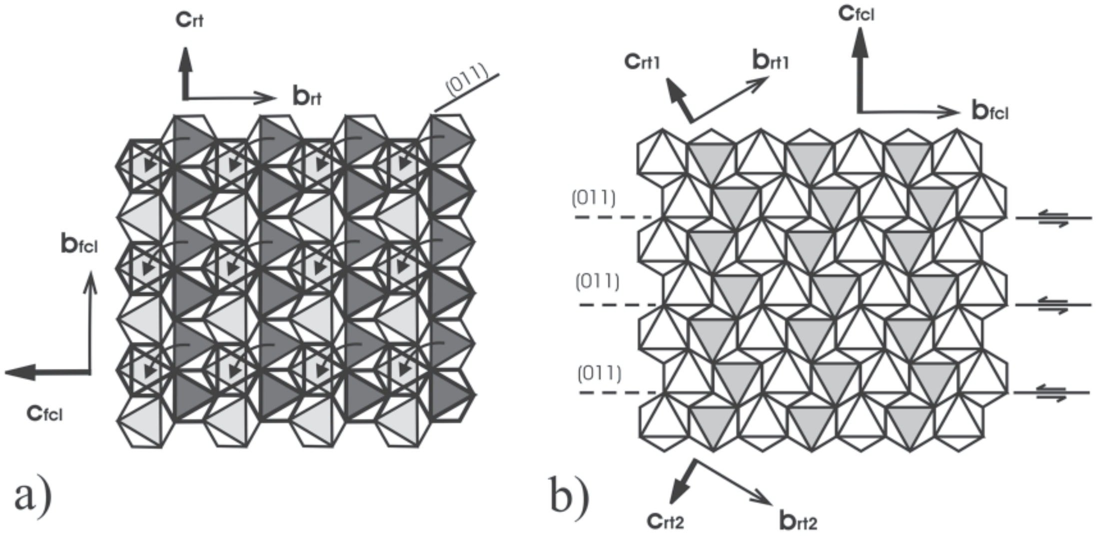

FIG. 7. Transformation of the rutile to the columbite structure a) by displacing every other cation of a chain running in the **c** direction in rutile to the nearest octahedral void, and b) by rutile twinning along (101), facilitated by shearing.

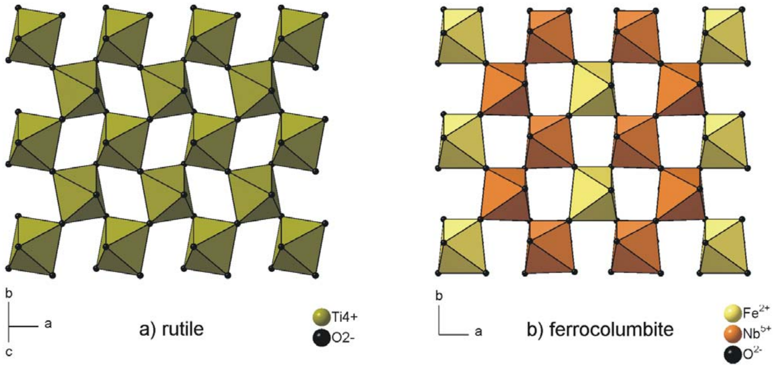

FIG. 8. Analogous arrangements of octahedra parallel to (011) of rutile (a) and (001) of ferrocolumbite (b).

growth are coarse, far past the nucleation stage, and their coherence with the host has long been lost.

To conclude, we propose the following scheme for the formation of ferrocolumbite lamellae within the rutile matrix (Fig. 9). First, the primary phase having the rutile structure was sheared to form twins along {101}, possibly at the time of shearing of the pegmatite during its emplacement. Second, disordered ferrocolumbite started to precipitate at the twin boundaries, so that (001) of ferrocolumbite was parallel to (101) of rutile. The transformation was facilitated by cation diffusion, and the newly formed columbite phase was stabilized by a large difference in the size of cations; ^{VI}Fe: 0.78 Å, ^{VI}Nb: 0.64 Å (Shannon & Prewitt 1969). Third, the columbite lamellae gradually coarsened, which resulted in a slight change of unit-cell parameters and created a stress along the phase boundary. Consequently, the lamellae partly lost their coherency with the rutile, a process accompanied by a rotation of the interface. In addition, some of the lamellae or the inner parts of the coarser lamellae ordered.

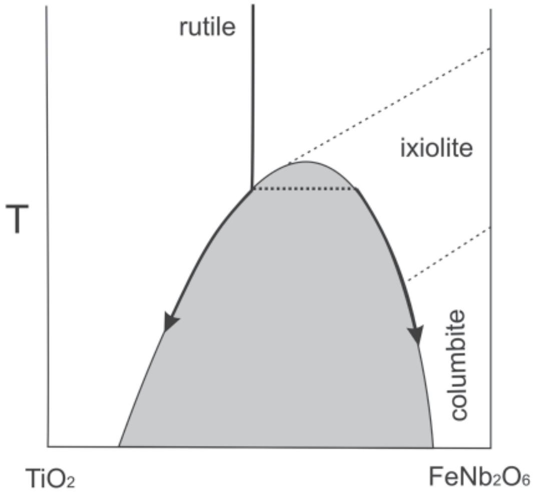

FIG. 9. A possible scheme illustrating the origin of rutile–ferrocolumbite intergrowths.

CLOSING REMARKS

This may well be the first documented case where the crystallographic orientation between the host rutile and ferrocolumbite precipitates has been determined. It is interesting that observations correspond to only one of the two possible orientations predicted by the theory of optimal phase-boundaries. In rutile from Košín, Czech Republic (Klementová & Rieder, unpubl. data), the reflections of the columbite-type phase are doubled and apparently correspond to both predicted solutions. More single-crystal research is in progress both on rutile and cassiterite (an identical structure), which may shed light on the problem.

We also attempted TEM observations. However, we encountered severe problems during sample preparation. The sample is too small to be ion-milled, and in crushed-grain samples, the lamellae were found to be invariably separated from rutile, which prevented imaging of the interface.

ACKNOWLEDGEMENTS

The material used was collected by Dr. J. Klomínský (Czech Geological Survey), who made it available for study. The laboratory research conducted at Charles University and at the Czech Geological Survey was supported by the Grant Agency of the Czech Republic (grant No. 205/01/1126) and the Grant Agency of Charles University (grant No. 198/2000 B GEO). The authors are indebted to Dr. J. Frýda (Czech Geological Survey) for performing the chemical analyses and to Dr. M.E. Fleet (University of Western Ontario, London, Ontario) for making available his program for the calculation of optimal phase-boundaries. Comments made by the reviewers significantly improved the quality of presentation of this paper.

REFERENCES

ARUGA, A., TOKIZAKI, E., NAKAI, I. & SUGITANI, Y. (1985): Structure of iron diniobium hexaoxide, $FeNb_2O_6$: an example of metal-disordered trirutile structure. *Acta Crystallogr.* **C41**, 663-665.

BAUMGARTE, A. & BLACHNIK, R. (1994): New $M^{2+}M^{4+}Nb_2O_8$ phases. *J. Alloys Compd.* **215**, 117-120.

BENDELIANI, N.A., POPOVA, S.V. & VERESHCHAGIN, L.F. (1966): New modification of titanium dioxide obtained at high pressures. *Geochem. Int.* **3**, 387-390.

BETTENAY, L.F., PARTINGTON, G.A., GROVES, D.I. & PATERSON, C. (1988): Nature and emplacement of the Giant rare-metal pegmatite at Greenbushes, Western Australia. *In* Proc. Seventh Quadrennial IAGOD Symp. E. Schweizerbart'sche Verlagsbuchhandlung, Stuttgart, Germany (401-408).

ČERNÝ, P. (1991): Rare-element granitic pegmatites. I. Anatomy and internal evolution of pegmatite deposits. *Geosci. Can.* **18**, 49-67.

________, ČECH, F. & POVONDRA, P. (1964): Review of ilmenorutile–strüverite minerals. *Neues Jahrb. Mineral., Abh.* **101**, 142-172.

________, CHAPMAN, R., GÖD, R., NIEDERMAYER, G. & WISE, M.A. (1989): Exsolution intergrowth of titanian ferrocolumbite and niobian rutile from the Weinebene spodumene pegmatites, Carinthia, Austria. *Mineral. Petrol.* **40**, 197-206.

________, ________, SIMMONS, W.B. & CHACKOWSKY, L.E. (1999): Niobian rutile from the McGuire granitic pegmatite, Park County, Colorado: solid solution, exsolution and oxidation. *Am. Mineral.* **84**, 754-763.

________, ERCIT, T.S., WISE, M.A., CHAPMAN, R. & BUCK, H.M. (1998): Compositional, structural and phase relationships in titanian ixiolite and titanian columbite–tantalite. *Can. Mineral.* **36**, 547-561.

________, NOVÁK, M., CHAPMAN, R. & MASAU, M. (2000): Subsolidus behavior of niobian rutile from Vežná, Czech Republic: a model for exsolution in phases with Fe^{2+} >> Fe^{3+}. *J. Czech Geol. Soc.* **45**(1-2), 21-35.

________, PAUL, B.J., HAWTHORNE, F.C. & CHAPMAN, R. (1981): A niobian rutile – disordered columbite intergrowth from the Huron Claim pegmatite, southeastern Manitoba. *Can. Mineral.* **19**, 541-548.

KUSABA, K., KIKUCHI, M., FUKOKA, K. & SYONO, Y. (1988): Anisotropic phase transition of rutile under shock compression. *Phys. Chem. Minerals* **15**, 238-245.

MEAGHER, E.P. & LAGER, G.A. (1979): Polyhedral thermal expansion in the TiO_2 polymorphs: refinement of the crystal structures of rutile and brookite at high temperature. *Can. Mineral.* **17**, 77-85.

NEIVA, A.M.R. (1996): Geochemistry of cassiterite and its inclusions and exsolution products from tin and tungsten deposits in Portugal. *Can. Mineral.* **34**, 745-768.

NICKEL, E.H., ROWLAND, J.F. & MCADAM, R.C. (1963): Ixiolite – a columbite substructure. *Am. Mineral.* **48**, 961-979.

PALMER, D.C., PUTNIS, A. & SALJE, E.K.H. (1988): Twinning in tetragonal leucite. *Phys. Chem. Minerals* **16**, 298-303.

PARTINGTON, G.A. (1990): Environment and structural controls on the intrusion of the giant rare metal Greenbushes pegmatite, Western Australia. *Econ. Geol.* **85**, 437-456.

ROBINSON, P., ROSS, M., NORD, G.L., JR., SMYTH, J.R. & JAFFE, H.W. (1977): Exsolution lamellae in augite and pigeonite: fossil indicators of lattice parameters at high temperature and pressure. *Am. Mineral.* **62**, 857-873.

SASAKI, T. (2002): Stability of rutile-type TiO_2 under high pressure. *J. Phys. Condens. Mat.* **14**, 10557-10562.

SATO, H., ENDO, S., SUGIYAMA, M., KIKEGAWA, T., SHIMOMURA, O. & KUSABA, K. (1991): Baddeleyite-type high-pressure phase of TiO_2. *Science* **251**, 786-788.

SEKI, H., ISHIZAWA, N., MIZUTANI, N. & KATO, M. (1984): High temperature structures of the rutile-type oxides, TiO_2 and SnO_2. *J. Ceram. Soc. Japan* **92**, 219-223.

SHANNON, R.D. & PREWITT, C.T. (1969): Effective ionic radii in oxides and fluorides. *Acta Crystallogr.* **B25**, 925-946.

SOLOMON, M. & GROVES, D.I. (1994): *The Geology and Origin of Australia's Mineral Deposits.* Clarendon Press, Oxford, U.K.

SWAMY, V., GALE, J.D. & DUBROVINSKY, L.S. (2001): Atomistic simulation of the crystal structures and bulk moduli of TiO_2 polymorphs. *J. Phys. Chem. Solids* **62**, 887-895.

URUSOV, V.S., KHISINA, N.R. & CHRISTY, A. (1996): Quasi-equilibrium behaviour of TiO_2–SnO_2 solid solutions at high pressures and temperatures: the influence of non-hydrostaticity. *Eur. J. Mineral.* **8**, 791-804.

WEITZEL, H. (1976): Kristallstrukturverfeinerung von Wolframiten und Columbiten. *Z. Kristallogr.* **144**, 238-258.

WENGER, M. & ARMBRUSTER, T. (1993): Phase relations of columbite- and rutile-type compounds in the system $NiNb_2O_6$–TiO_2. *Neues Jahrb. Mineral., Monatsh.*, 224-232.

WITHERS, A.C., ESSENE, E.J. & ZHANG, YOUXUE (2003): Rutile/TiO_2 II phase equilibria. *Contrib. Mineral. Petrol.* **145**, 199-204.

Received November 28, 2003, revised manuscript accepted September 18, 2004.